

*Supporting information*

**Energy frameworks and a topological analysis of the supramolecular features in situ cryo-cryocrySTALLIZED liquids: Tuning the Weak Interaction Landscape by fluorination**

Dhananjay Dey<sup>a</sup>, Subhrajyoti Bhandary<sup>a</sup>, Sajesh P. Thomas<sup>b</sup>, Mark A. Spackman<sup>b</sup> and Deepak Chopra<sup>a\*</sup>

<sup>a</sup>Crystallography and Crystal Chemistry Laboratory, Department of Chemistry, Indian Institute of Science Education and Research Bhopal, Bhopal By-Pass Road, Bhauri, Bhopal-462066, Madhya Pradesh, India. E-mail: [dchopra@iiserb.ac.in](mailto:dchopra@iiserb.ac.in); Fax: +91 755 6692392

<sup>b</sup>School of Chemistry and Biochemistry, The University of Western Australia, Crawley, WA, Australia. E-mail: mark.spackman@uwa.edu.au; Fax: +61 8 6488 7330

**Table S1.** Conditions (laser intensities and temperatures) for the crystallization

Compound	Temperature	Ramp rate	Laser intensity		
			Output	Main	Fine
3-Fluorobenzoyl chloride (Sigma Aldrich)	230K	70K/h	---	---	---
3,5-Difluorobenzoyl chloride (Sigma Aldrich)	245K	70K/h	35.2	12.2%	2.4%
3,4,5-Trifluorobenzoyl chloride (Sigma Aldrich)	180K	70K/h	44	16.9%	22.4%

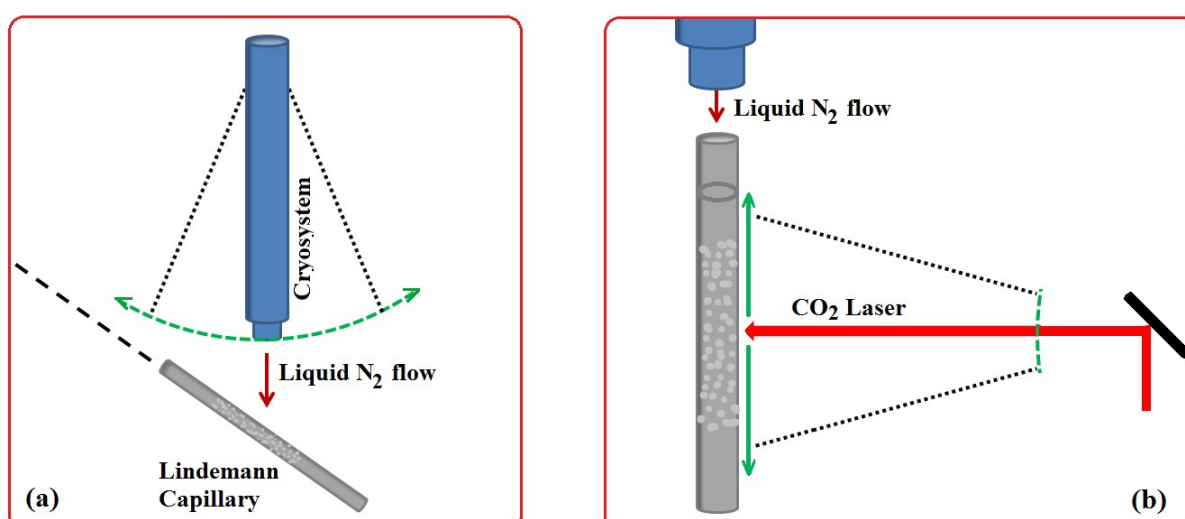


**Figure S1.** Crystallization procedures: (a) manual crystallization and (b) crystallization using CO<sub>2</sub> laser in OHCD.

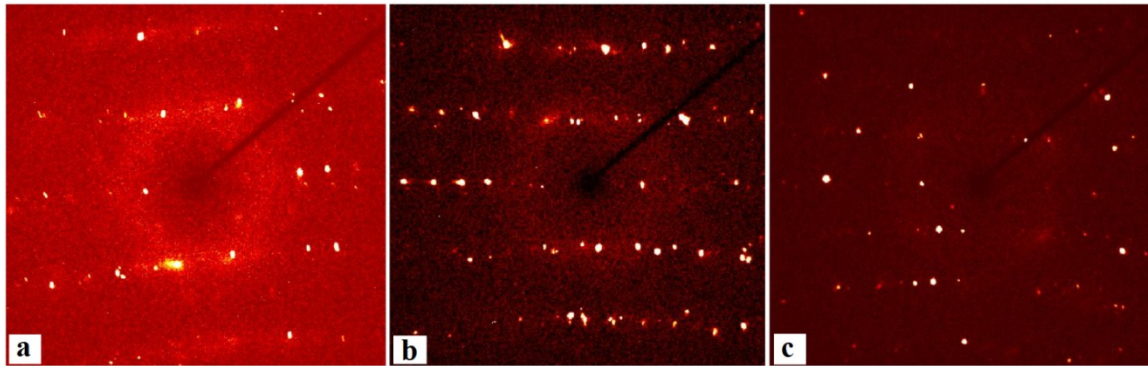


**Figure S2:** Diffraction (still) images of (a) 3FBC and (b) 35DFBC and 345TFBC.

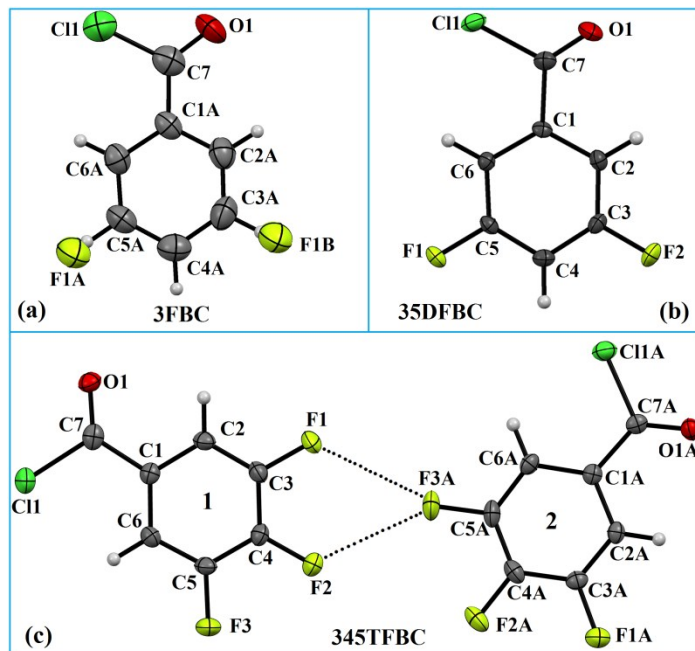


**Figure S3.** *ORTEP* diagrams of (a) 3FBC, (b) 35DFBC and (c) 345TFBC drawn with 50% ellipsoidal probability.

#### Data collections and details of structure refinement

All the single crystal diffraction data have been collected using a Bruker APEX II diffractometer equipped with a CCD detector using monochromated Mo K $\alpha$  radiation ( $\lambda = 0.71073 \text{ \AA}$ ). The unit cell measurement, data collection, integration, scaling and absorption corrections for these forms were done using Bruker Apex II software [1]. The intensity data were processed by using the Bruker SAINT [2] suite of programs. The crystal structures were solved by direct methods using SIR 92 [3] and refined by the full matrix least squares method using SHELXL 2014 [4] present in the program suite WinGX (version 2014.1) [5]. Empirical

absorption correction was applied using SADABS [6]. The non-hydrogen atoms were refined anisotropically and the hydrogen atoms bonded to C atom, were positioned geometrically and refined using a riding model with  $U_{\text{iso}}(\text{H}) = 1.2U_{\text{eq}}$ . The crystal packing diagrams were generated using Mercury 3.5.1 (CCDC) program [7]. Geometrical calculations were done using PARST [8] and PLATON [9].

The occupancies of the disordered fluorine (attached at *meta* position of the phenyl ring) at the two positions were refined using the part command namely F1A (55%) and F1B (45%). The anisotropic displacement parameters were fixed using EADP command. All the theoretical calculations were performed taking the atomic coordinates of the major part A.

**Table S2.** Data collections and structure refinements

Sample code	3FBC	35DFBC	345TFBC
Formula	$\text{C}_7\text{H}_4\text{ClFO}$	$\text{C}_7\text{H}_3\text{ClF}_2\text{O}$	$\text{C}_7\text{H}_2\text{ClF}_3\text{O}$
Formula weight	158.55	176.54	194.54
Temperature/K	230(2)	110(2)	110(2)
Wavelength (Å)	0.71073	0.71073	0.71073
CCDC number	1498349	1426055	1452041
Crystal system	Monoclinic	Monoclinic	Monoclinic
Space group	$P2_1/n$	$P2_1/c$	$P2_1/c$
<i>a</i> (Å)	3.8275(5)	3.7798(4)	13.4138(5)
<i>b</i> (Å)	10.9838(12)	18.1130(13)	5.1617(2)
<i>c</i> (Å)	16.3303(16)	10.0510(8)	20.5882(7)
$\alpha$ (°)	90	90	90
$\beta$ (°)	95.919(8)	95.479(4)	97.546(2)
$\gamma$ (°)	90	90	90
$V(\text{\AA}^3)$	682.87(13)	684.98(10)	1413.14(9)
$Z'$	1	1	2
$Z$	4	4	8
Density(g cm <sup>-3</sup> )	1.542	1.712	1.829
$\mu$ (mm <sup>-1</sup> )	0.495	0.523	0.536
F (000)	320	352	768
$\theta$ (min, max)	2.31, 25.60	2.25, 30.30	2.35, 30.29
Treatment of hydrogens	Fixed	Fixed	Fixed
$h_{\text{min, max}}, k_{\text{min, max}}, l_{\text{min, max}}$	(-2, 4), (-13, 12), (-18, 19)	(-2, 2), (-23, 23), (-13, 13)	(-15, 15), (-4, 4), (-27, 27)
No. of ref.	4570	18253	8734
No. of unique ref./ obs. Ref.	1139, 841	1110, 1049	2319, 2088
No. parameters	95	100	217
R_all, R_obs	0.1096, 0.0869	0.0296, 0.0079	0.0328, 0.0296
wR <sub>2</sub> _all, wR <sub>2</sub> _obs	0.2332, 0.2187	0.0870, 0.0840	0.0820, 0.0798
$\Delta\rho_{\text{min, max}}(\text{e\AA}^{-3})$	-0.275, 0.340	-0.242, 0.261	-0.319, 0.259
G. o. F.	1.079	1.081	1.127

### PIXEL and QTAIM analysis

The dimer interaction energies associated with the presence of various non-covalent interactions present in the crystal packing were estimated using PIXEL (version 12.5.2014)

[10-12] program. The electron densities were calculated using Gaussian 09 program [13] at MP2/6-31G\*\* level to generate the required PIXEL input. The total lattice energy of the molecule is classified into the corresponding Coulombic, polarization, dispersion and repulsion energies.

The electrostatic contribution to the total stabilization of a particular molecular pair

$$= [(E_{\text{Coul}} + E_{\text{Pol}}) / (E_{\text{Coul}} + E_{\text{Pol}} + E_{\text{Disp}})] \times 100\%.$$

The dispersion contribution to the total stabilization of a particular molecular pair

$$= [E_{\text{Disp}}) / (E_{\text{Coul}} + E_{\text{Pol}} + E_{\text{Disp}})] \times 100\%.$$

QTAIM analysis for some selected dimers at the crystal geometry (with the hydrogen atoms moved to their neutron value) was performed at the MP2/6-311++G\*\* level using Gaussian 09. The formatted checkpoint file (fchk) was used as input file for AIMALL (version 13.05.06) [14] calculation. The electron density features at the bond critical points, which are computed, is as follows: (i) electron density ( $\rho_b$ ), (ii) Laplacian ( $\nabla^2\rho_b$ ), (iii) local potential energy ( $V_b$ ), and (iv) kinetic energy density ( $G_b$ ). The dissociation energies for the different intermolecular interactions were determined using the empirical approach: (i)  $E_{\text{int}} = -0.5V_b$  (in au) [15-16].

**Table S3.** Stabilization energies (in kcal/mol) of the individual molecular pairs associated with different intermolecular interactions [**1** and **2** represent the symmetry independent molecules present in the asymmetric unit respectively]

I	x+1, y, z	3.828	-0.2	-0.5	-6.7	3.9	-3.6	Cg1···Cg1	3.828(1)
II	-x+3/2, y-1/2, -z+1/2	6.316	-1.3	-0.5	-2.5	1.4	-3.0	C6A-H6A···O1 C2A-H2A···Cl1	2.82, 121 2.89, 149
III	x-1/2, -y+1/2, z+1/2	8.707	-1.5	-0.3	-1.9	1.0	-2.8	C4A-H4A···O1	2.73, 172
IV	-x+1/2, y-1/2, -z+1/2	5.870	-0.2	-0.3	-3.1	1.3	-2.3	O1···F1A C6A-H6A···O1 C2A-H2A···Cl1	2.957(7) 3.07, 120 3.21, 113
V	-x, -y, -z+1	8.543	-0.6	-0.1	-1.7	1.9	-0.5	F1A···F1A C4A-H4A···F1A	2.664(10) 2.76, 120
4FBC									
I	x, -y+1/2, z+1/2	4.275	-1.5	-0.5	-6.8	5.1	-3.7	Cg1···Cg1	3.760(1)
II	1-x, y-1/2, -z+1/2	7.288	-1.1	-0.4	-2.6	1.4	-2.7	C6-H6···F1 C5-H5···Cl1	2.54, 125 3.03, 171
III	-x, y-1/2, -z-1/2	7.441	-1.8	-0.6	-2.0	1.9	-2.5	C3-H2···O1 C2-H3···O1	2.55, 120 2.60, 118
IV	x, 1+y, z	9.113	-0.9	-0.2	-1.6	1.2	-1.5	F1···Cl1	3.153(1)
23DFBC									
I	-x, -y+1, -z+1	4.074	-2.7	-0.8	-7.6	5.8	-5.3	Cg1···Cg1	3.707(3)
II	-x+1, -y+2, -z+1	4.808	-1.2	-0.4	-6.3	4.1	-3.8	Cg1···Cg1	3.763(3)
III	x, y, z-1	8.037	-2.6	-0.5	-2.0	1.8	-3.3	C4-H4···O1 C5-H5···O1	2.55, 121 2.61, 120
IV	-x+1, -y+2, -z+2	5.573	-0.9	-0.4	-3.4	1.8	-2.9	Cl1···F1 $\pi(C=O)\cdots\pi(C=O)$	3.480(1) 3.323(2)
V	-x, -y+2, -z+1	6.529	-1.4	-0.2	-2.5	1.3	-2.8	F2···F2 F2···F1	3.060(2) 2.979(2)
VI	x+1, y, z	6.859	-0.8	-0.4	-2.8	2.2	-1.8	C6-H6···F1 C5-H5···F2 C6-H6···F2 Cl1···F1	2.60, 163 2.56, 124 2.77, 116 3.167(1)
VII	x+1, y, z+1	9.189	0.2	-0.2	-1.5	0.8	-0.7	Cl1···F2 C4-H4···Cl1	3.443(1) 3.08, 138
24DFBC									
I	x-1, y, z	3.829	-0.6	-0.8	-7.7	5.3	-3.8	Cg1···Cg1	3.829(2)
II	x-1/2, -y+1/2, z+1/2	6.622	-2.4	-0.6	-2.3	2.0	-3.3	C5-H5···O1 C6-H6···F1	2.69, 150 2.42, 127
III	-x+3/2, y-1/2, -z + 1/2	7.779	-1.0	-0.4	-2.0	1.0	-2.4	F2···O1 C3-H3···Cl1	3.116(2) 3.02, 134
IV	-x+1/2, y-1/2, -z + 1/2	7.794	-0.7	-0.3	-1.9	1.0	-1.9	F2···O1 C3-H3···Cl1	3.060(2) 3.10, 145
V	x+1/2, -y+1/2, z+1/2	6.251	-0.3	-0.2	-2.0	0.6	-1.9	C6-H6···F1	2.53, 124
VI	-x, -y+1, -z+1	9.045	-0.6	-0.2	-1.5	0.8	-1.5	C5-H5···F2 F2···F2	2.61, 136 3.159(2)
VII	-x+1, -y, -z+1	8.789	-0.8	-0.3	-2.0	2.0	-1.1	Cl1···Cl1	3.434(1)
VIII	-x+2, -y, -z+1	9.322	-0.5	-0.2	-1.4	1.1	-1.0	Cl1···Cl1	3.629(1)
25DFBC									
I (1-2)	-x+2, -y+1, -z+1	4.275	-1.7	-0.5	-6.7	4.0	-4.9	Cg1···Cg1'	3.779(3)
II (1-2)	-x+1, -y+1, -z+1	4.351	-2.0	-0.5	-7.0	4.7	-4.8	Cg1···Cg1'	3.726(4)
III (2-2)	-x-1, -y, -z+1	5.509	-2.3	-0.3	-3.5	1.8	-4.3	F1A···F1A O1A···F1A	2.949(2) 3.040(2)
IV (1-1)	-x+2, -y+1, -z+1	5.562	-2.1	-0.3	-3.3	1.6	-4.1	F1···F1 O1···F1	2.953(2) 3.038(2)
V (1-2)	x+1, y+1, z+1	6.620	-1.0	-0.5	-3.4	2.0	-2.9	C6A-H6A···F2 C6-H6···Cl1A	2.44, 145 2.82, 156
VI (2-2)	x, y+1, z	8.565	-1.7	-0.4	-2.0	1.2	-2.9	C4A-H4A···O1A Cl1A···F2A	2.57, 165 3.483(2)
VII (1-1)	x, y+1, z	8.565	-1.4	-0.4	-2.0	1.2	-2.6	C4-H4···O1 Cl1···F2	2.60, 164 3.512(2)

VIII (1-2)	x, y, z	7.431	-1.8	-0.8	-2.4	2.7	-2.3	C3A-H3A···O1 C3A-H3A···F1	2.55, 143 2.27, 131
IX (2-2)	-x+1, -y, -z	5.468	-0.1	-0.3	-3.7	2.0	-2.1	C1A···F2A	3.346(2)
X (1-2)	x, y+1, z	7.463	-1.5	-0.7	-2.3	2.5	-2.0	C3-H3···F1A C3-H3···O1A	2.26, 131 2.63, 141
XI (1-1)	-x+2, -y+1, -z+2	6.828	-0.7	-0.2	-2.2	1.1	-2.0	C11···C11	3.743(1)
XII (A-A)	-x+2, -y+2, -z+2	7.050	-0.4	-0.1	-1.6	0.5	-1.6	F2···F2	3.061(2)
XIII (1-2)	x+1, y, z+1	8.892	-0.2	-0.1	-1.0	1.0	-0.3	C11···F2A	3.106(2)

### 26DFBC

I(1-2)	-x+1, y-1/2, -z+3/2	4.642	-2.6	-0.8	-7.6	5.4	-5.6	Cg1···Cg1'	3.692(2)
II(2-2)	-x+2, -y+1, -z+1	5.684	-2.7	-0.6	-3.6	2.1	-4.8	F1A···F1A C3A-H3A···O1A	2.992(2) 2.78, 109
III(1-1)	x, -y+1/2, z+1/2	5.977	-1.7	-0.4	-3.1	1.5	-3.7	C5-H5···O1 F1···F2	2.82, 119 2.815(1)
IV (2-2)	-x+2, y-1/2, -z+3/2	7.973	-2.6	-0.7	-2.6	2.3	-3.6	C5A-H5A···O1A C4A-H4A···C1A	2.44, 139 2.96, 144
V(1-1)	-x+1, y-1/2, -z+3/2	8.140	-2.3	-0.6	-2.4	2.0	-3.3	C4-H4···O1 C3-H3···C11	2.45 139 3.11, 135
VI(1-2)	-x+2, y-1/2, -z+3/2	5.566	-1.3	-0.4	-5.1	3.6	-3.2	Cg1···Cg1'	3.831(3)
VII(1-2)	x, y, z	5.783	-1.2	-0.5	-3.3	2.5	-2.5	F2···C11A	3.383(1)
VIII(1-2)	x, -y+1/2, z+1/2	7.635	-1.0	-0.4	-2.0	1.4	-2.0	C5-H5···F1A C4-H4···F1A	2.67, 115 2.44, 125
IX(1-2)	x-1, y, z	6.180	-0.4	-0.2	-2.3	1.2	-1.7	C11···C11A	3.698(1)
X(1-2)	-x+1, -y+1, -z+1	7.526	-0.4	-0.3	-1.5	1.1	-1.1	C3A-H3A···F1	2.34, 145
XI(2-2)	-x+2, -y+1, -x+2	6.926	-0.6	-0.4	-2.9	3.0	-0.9	C11A···F2A	3.157(1)

### 35DFBC

I	x-1, y, z	3.780	-1.0	-0.7	-7.8	5.7	-3.8	Cg1···Cg1	3.780(3)
II	x, -y+1/2, z-1/2	6.284	-0.3	-0.2	-2.7	1.0	-2.2	F1···C11	3.597(1)
III	x-1, -y+1/2, z-1/2	7.081	-1.4	-0.5	-2.2	2.0	-2.1	C6-H6···O1	2.35, 146
IV	-x-1, -y+1, -z+1	8.320	-1.3	-0.3	-2.0	1.5	-2.1	C4-H4···F1 F1···F1	2.45, 135 3.116 (2)
V	-x, y-1/2, -z+3/2	9.070	-0.9	-0.3	-1.8	1.1	-1.9	C11···F2 C4-H4···C11	3.316(1) 2.96, 137
VI	-x+1, -y+1, -z+2	7.677	-0.9	-0.2	-1.7	1.0	-1.8	C2-H2···F2	2.54, 138
VII	-x, -y+1, -z+2	7.181	-0.6	-0.1	-2.0	0.9	-1.8	F2···F2	3.031(2)

### 345TFBC

I(2-2)	-x+2, y-1/2, -z+3/2	6.853	-3.1	-0.8	-3.7	3.6	-4.1	C2A-H2A···O1A O1A···C7	2.42, 176 3.037(2)
II(1-2)	-x+1, -y+1, -z+1	4.949	-1.0	-0.6	-5.6	3.6	-3.7	C7=O1···(C1A-C6A) C11···C11A C1···C7A	3.285(3) 3.696(3) 3.624(3)
III(1-1)	x, y-1, z	5.162	-0.8	-0.5	-5.0	2.8	-3.6	C7···π(C4-C5) π(C=O)···π(C3-C4)	3.367(3) 3.396(3)
IV(1-2)	-x+1, -y, -z+1	7.723	-1.8	-0.6	-3.0	3.0	-2.5	C11···C11A C6A-H6A···O1	3.479(1) 2.54, 152
V(1-2)	x+1, y+1, z	7.543	-0.9	-0.4	-3.0	2.0	-2.3	C6-H6···C11A F3···O1A	2.97,150 3.175(2)
VI(1-1)	-x, -y, -z+1	7.370	-0.4	-0.2	-2.6	1.0	-2.3	C6-H6···C11	3.18, 135
VII(2-2)	x, y-1, z	5.162	-0.2	-0.4	-4.8	3.1	-2.3	C3A···C6A	3.532(3)
VIII(1-2)	x, y+1, z	6.911	-0.7	-0.1	-2.3	1.0	-2.1	F1···F2A F2···F2A	2.995(2) 2.975(2)
IX(1-1)	-x+1, -y, -z+1	6.877	-0.5	-0.5	-2.9	2.0	-1.8	C2-H2···F1	2.38, 174
X(1-2)	-x+1, y+1/2, -z+3/2	5.992	-0.4	-0.2	-2.4	1.2	-1.8	F2···F1A C5-F3···C2A	3.079(2) 3.143(3)

XI(1-2)	$-x+1, y-3/2, -z+3/2$	6.119	-0.4	-0.1	-1.7	0.9	-1.3	F1A $\cdots$ F2A F2A $\cdots$ F2A	3.065(2) 3.306(2)
XII(1-1)	$-x, -y-1, -z+1$	9.539	-1.4	-0.6	-2.4	3.8	-0.9	Cl1 $\cdots$ Cl1	3.274(1)
XIII(1-2)	x, y, z	8.537	0.1	0.0	-0.8	0.2	-0.5	F2 $\cdots$ F3A F1 $\cdots$ F3A	2.973(2) 3.006(2)

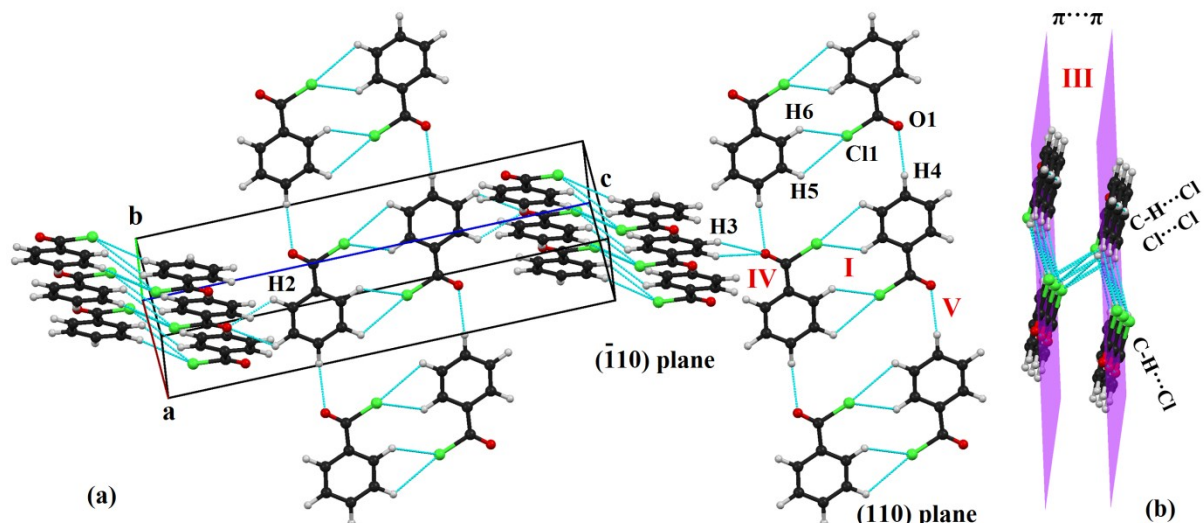


**Figure S4.** Crystal packing of BC (a) formation of a similar types of alternate molecular [down the  $(110)$  plane and  $(1-10)$  plane] sheets associated with weak  $\text{C}-\text{H}\cdots\text{O}$ ,  $\text{C}-\text{H}\cdots\text{Cl}$  interactions (b) parallel molecular sheets connected *via*  $\text{C}-\text{H}\cdots\text{Cl}$  and  $\text{Cl}\cdots\text{Cl}$  interaction.

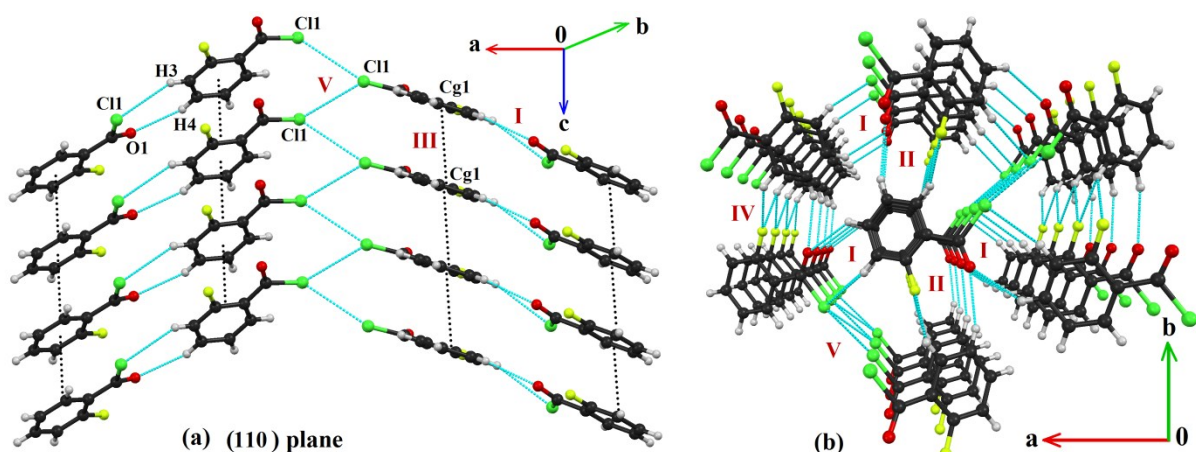


**Figure S5.** Packing network of 2FBC showing (a) intermolecular  $\text{Cl}\cdots\text{Cl}$  zigzag chain along  $c$  axis down the  $(110)$  plane; (b) down the  $ab$  plane formation of molecular sheets (associated with the molecular pairs I, II, IV and V) stacked on each other along  $c$  axis.

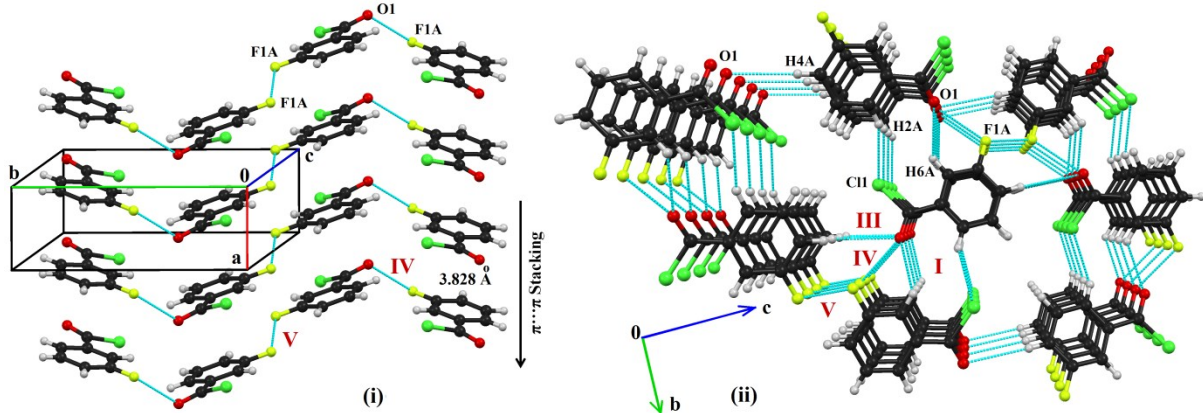


**Figure S6a.** Crystal packing of **3FBC** (i) depicting the molecular chains (connected with intermolecular  $F\cdots O$  and  $F\cdots F$  contact) stacked on each other along the *a* axis; (ii) molecular sheet associated with weak intermolecular  $C-H\cdots O$ ,  $C-H\cdots Cl$ ,  $F\cdots O$  and  $F\cdots F$  interactions down the *bc* plane.

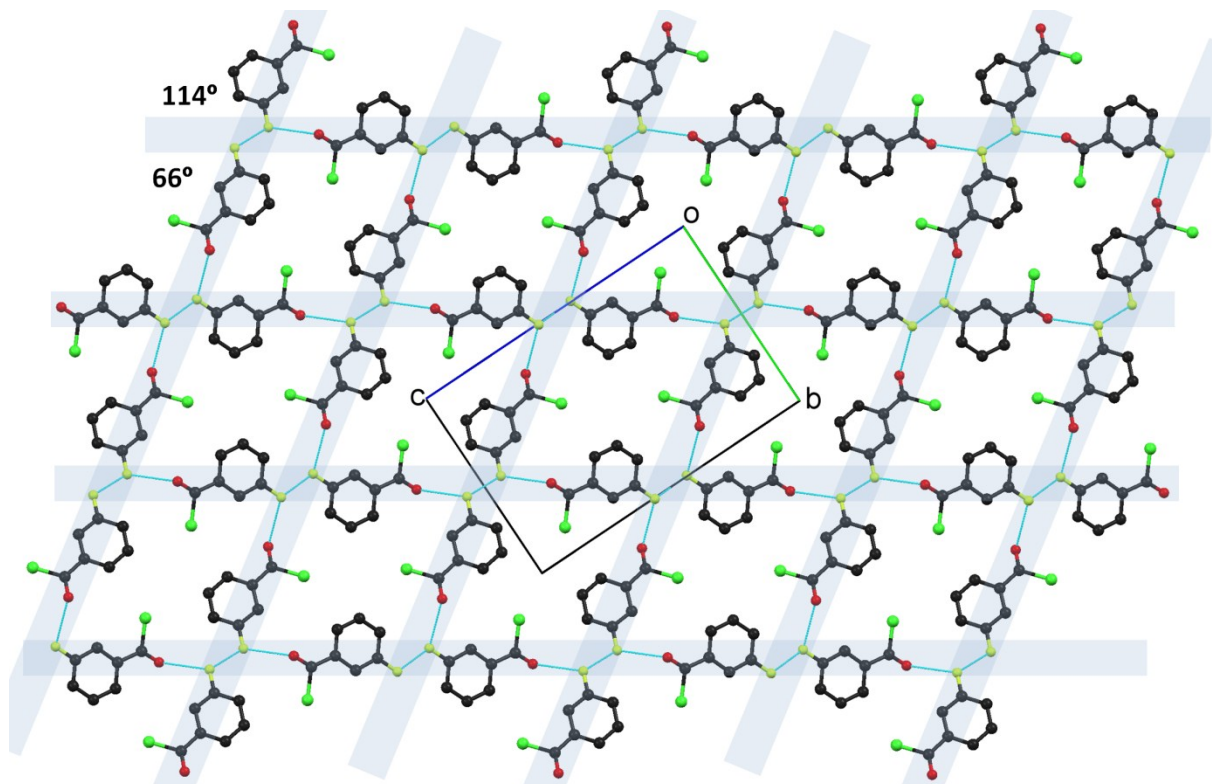


**Figure S6b.** Molecular sheet down the *bc* plane involving the molecular chains (transparent sky blue colour) associated with intermolecular  $F\cdots F$  and  $F\cdots O$  interaction in **3FBC**.

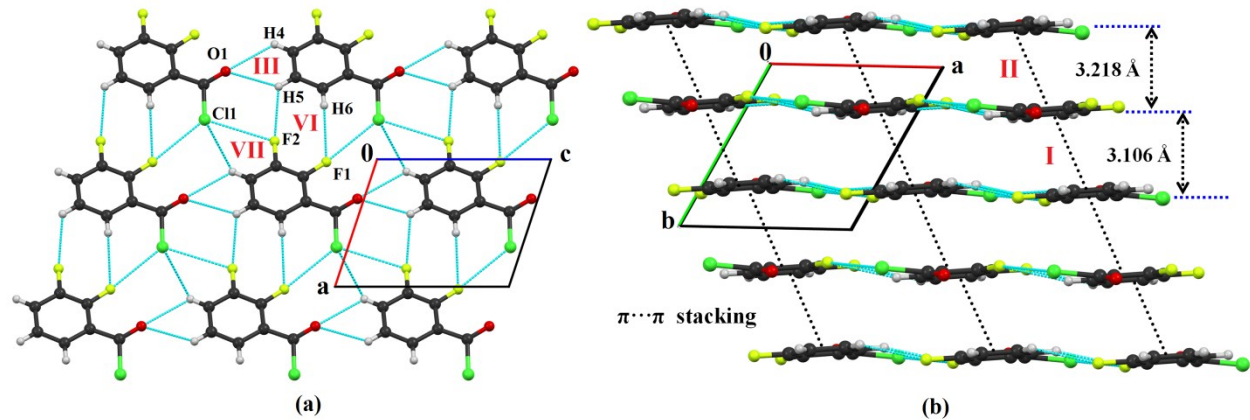


**Figure S7.** Packing view of **23DFBC** (a) down the *ac* plane; formation of molecular sheet associated with weak C-H···O, C-H···F, C-H···Cl and Cl···F contacts and (b) layers of sheets parallel to each other interacts *via*  $\pi\cdots\pi$  stacking.

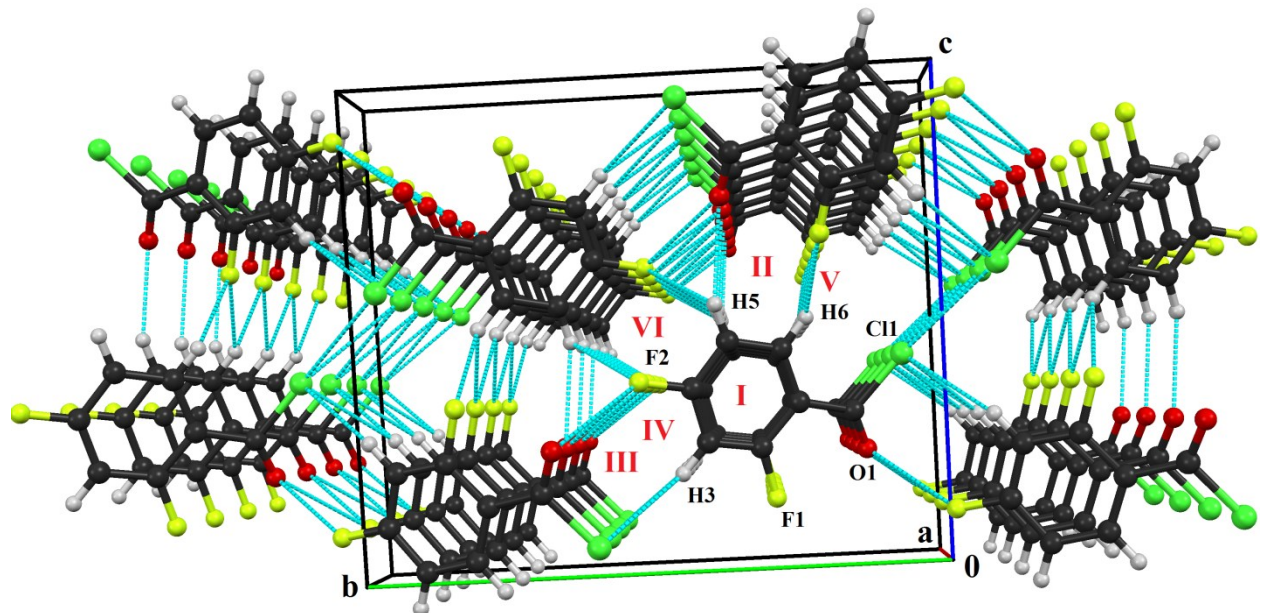


**Figure S8.** Packing network of **24DFBC** shows the formation of molecular sheet associated with C-H···F dimer, weak C-H···Cl, C-H···O interaction, F···O contact and zigzag Cl···Cl interaction along with the molecular stacking.

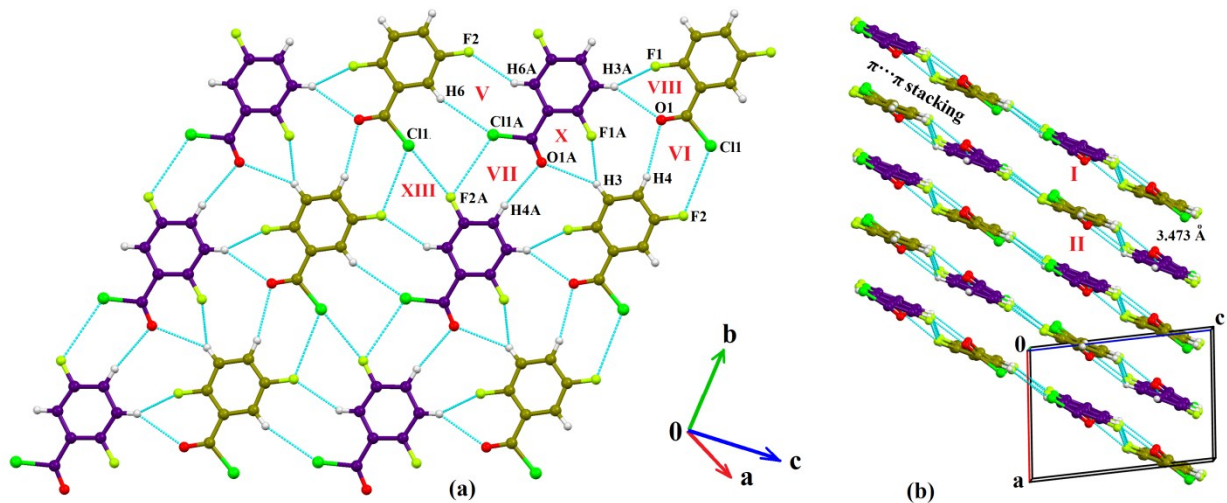


**Figure S9.** Packing network of **25DFBC** (**25DFBC-1**: olive color, **25DFBC-2**: indigo color) showing (a) the molecular sheet down the (101) plane associated with weak C-H···O, C-H···F, C-H···Cl interactions and Cl···F contact; (b) molecular stacking between the molecular sheets.

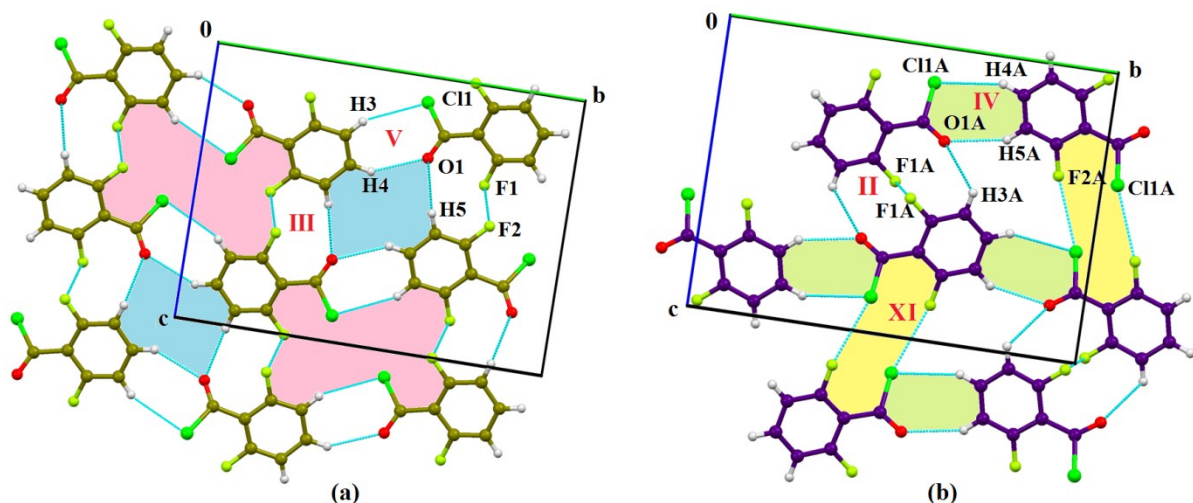


**Figure S10a.** Packing network of **26DFBC** formation of molecular sheets (a) between **26DFBC\_1** and ; (b) molecules **26DFBC-2** down the *bc* plane.

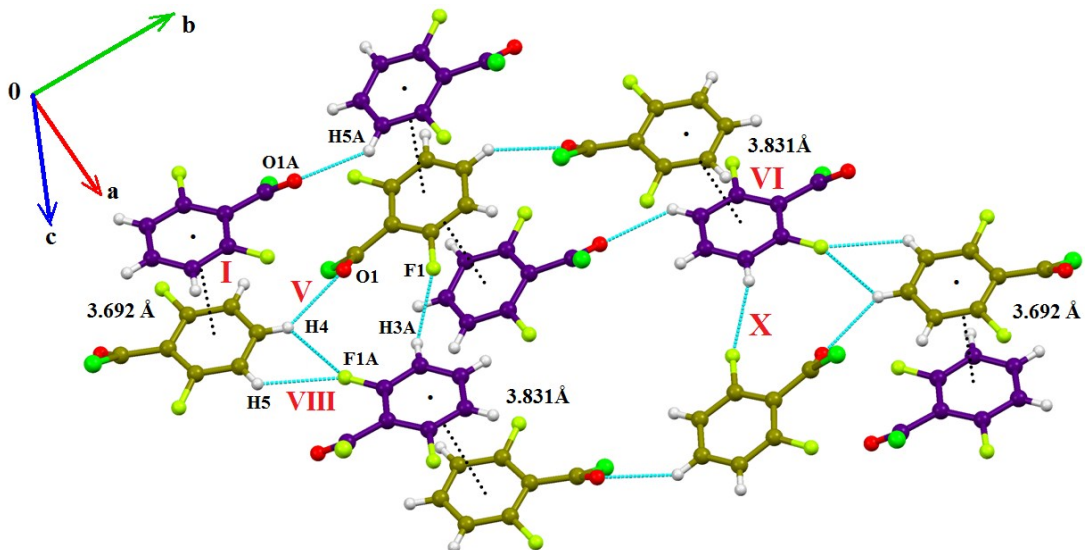


**Figure S10b.** Crystal packing of **26DFBC** involving molecules **A** and **B** associated with  $\pi \cdots \pi$  stacking and weak C-H $\cdots$ F and C-H $\cdots$ O intermolecular interactions.

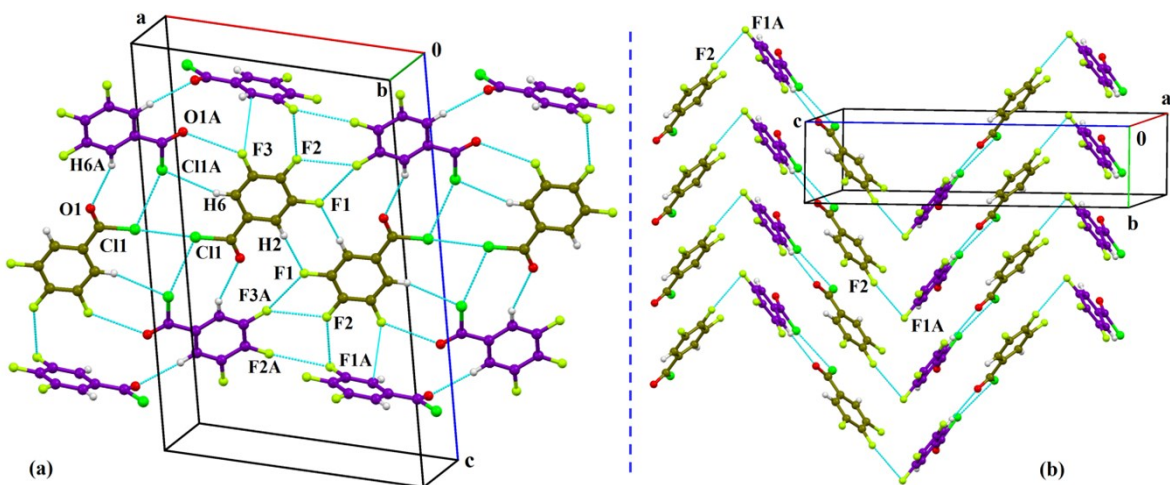


**Figure S11.** The packing network of **345TFBC** showing (a) the molecular sheet along *a* direction associated with two symmetry independent molecules attached *via* weak intermolecular F $\cdots$ F, Cl $\cdots$ Cl, C-H $\cdots$ F, C-H $\cdots$ Cl, C-H $\cdots$ O and F $\cdots$ O interaction down the *ac* plane; (b) zig-zag molecular chains connected *via* molecular stacking.

### Energy framework analysis

The energy framework analysis [Reference number 57(a) in the main manuscript] introduced by Spackman *et al.*, provides a means to visualize the intermolecular interaction topology in molecular crystals. The pairwise intermolecular interaction energies are computed using an

approach described in [Reference number 57(b) in the main manuscript]. These energies are estimated from B3LYP/6-31G(d,p) molecular wave functions calculated at the crystal geometry, summing up the electrostatic, polarization, dispersion and exchange-repulsion terms based on a scaling scheme.

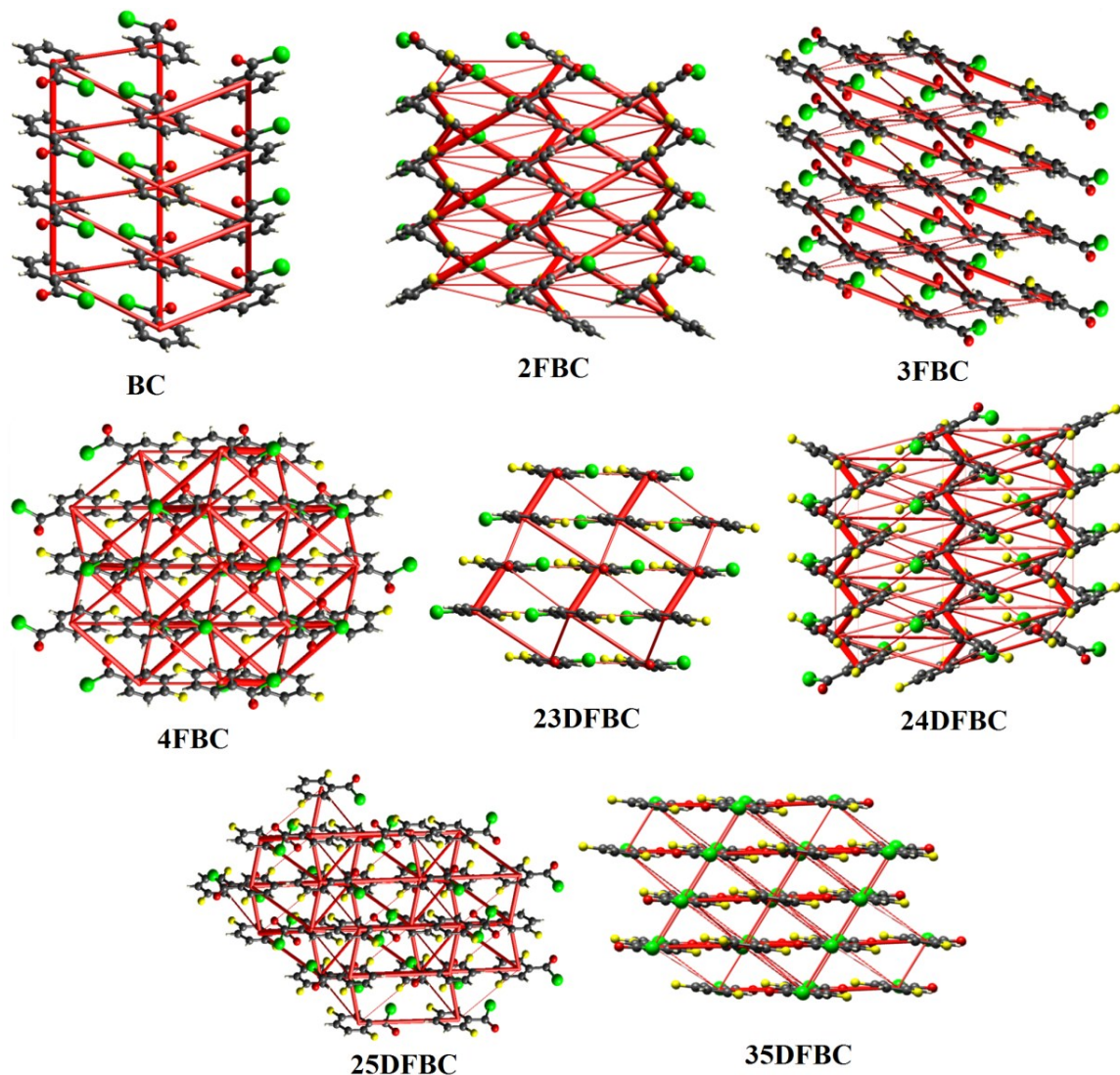


**Figure S12.** Electrostatic components of the energy framework for the fluorinated benzoyl chlorides.

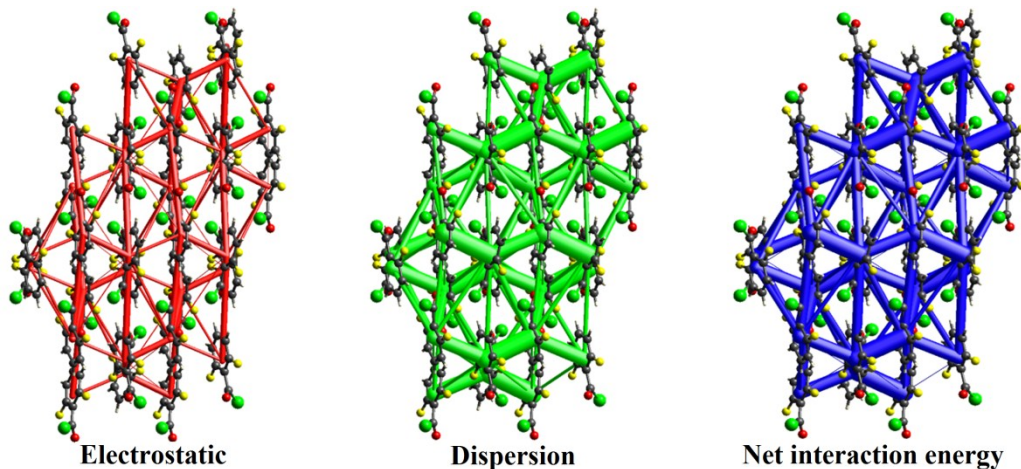


**Figure S13.** Energy framework of **26DFBC** viewed down the crystallographic *c* axis.

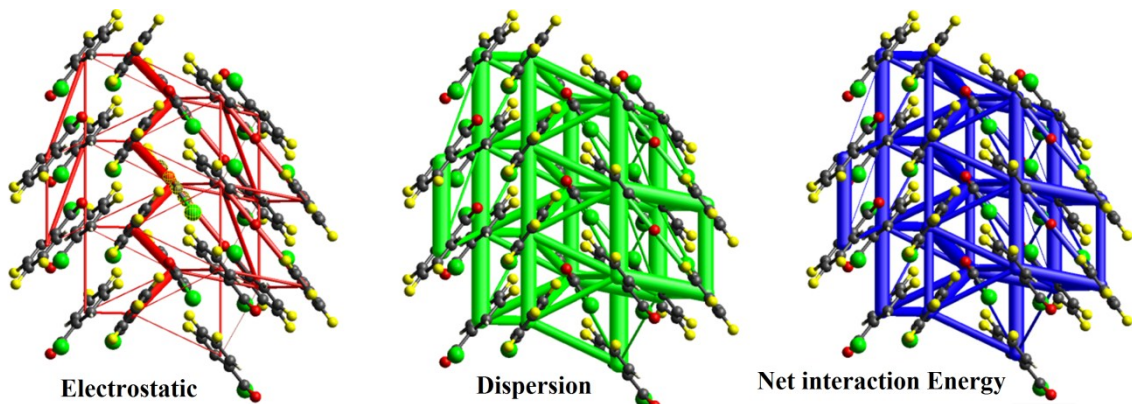


**Figure S14.** Energy framework of **345TFBC** viewed down the crystallographic *c* axis.

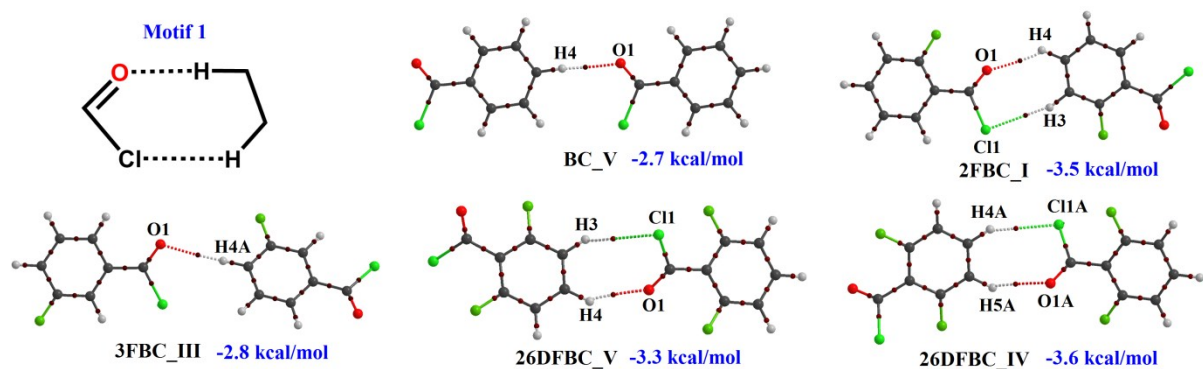


**Figure S15a.** Molecular graphs for the **Motif 1** associated with C-H...O and C-H...Cl interactions.

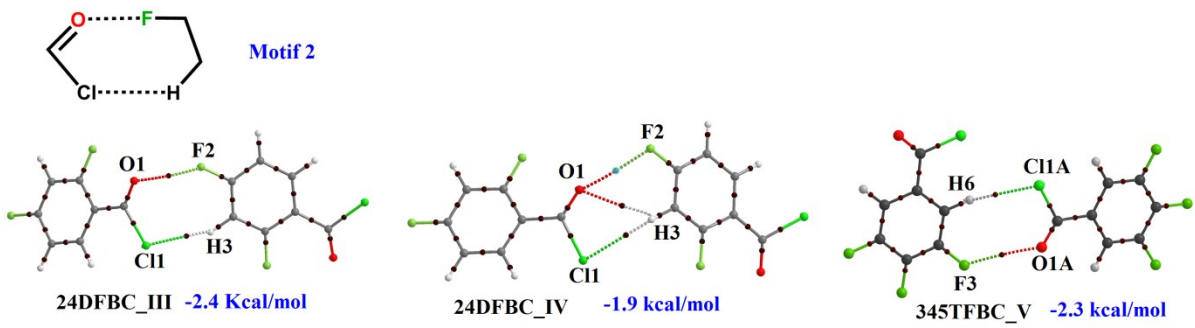


**Figure S15b.** Molecular graphs for the **Motif 2** associated with C-H $\cdots$ Cl interaction and intermolecular F $\cdots$ O contact.

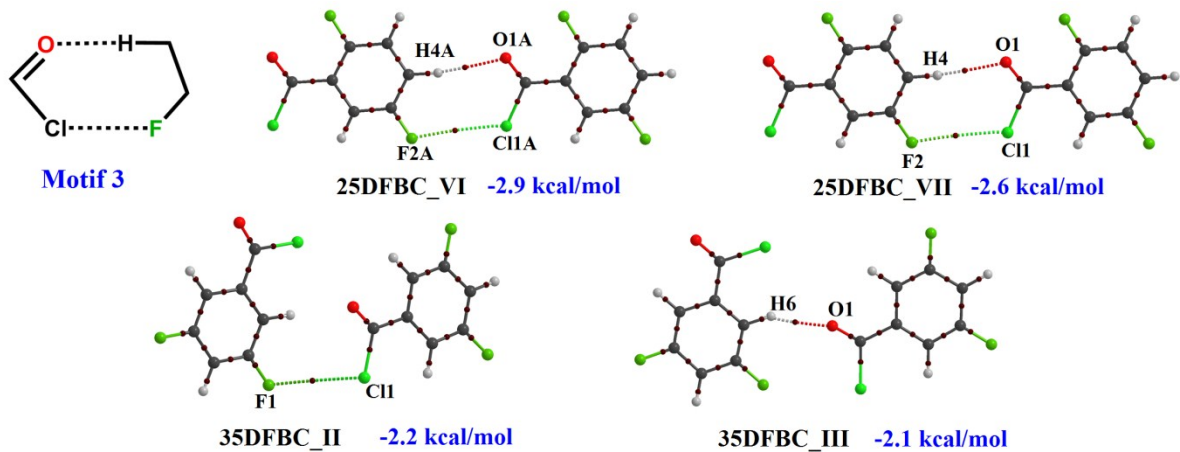


**Figure S15c.** Molecular graphs for the **Motif 3** associated with C-H $\cdots$ O and intermolecular Cl $\cdots$ F contact.



**Figure S15d.** Molecular graphs for the **Motif 4** associated with C-H $\cdots$ Cl and C-H $\cdots$ O interactions.

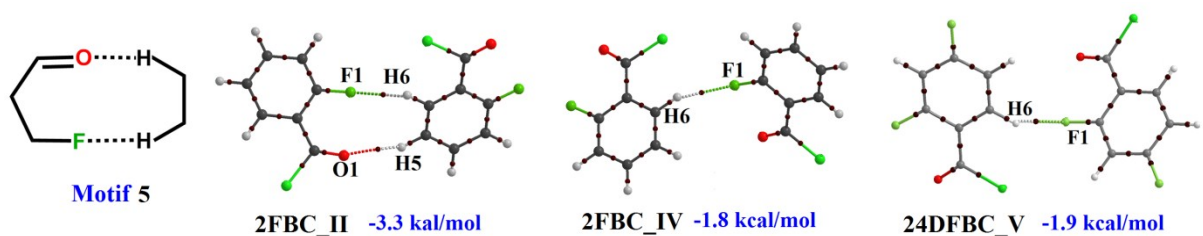


**Figure S15e.** Molecular graphs for the **Motif 5** associated with C-H···F and C-H···O interactions.

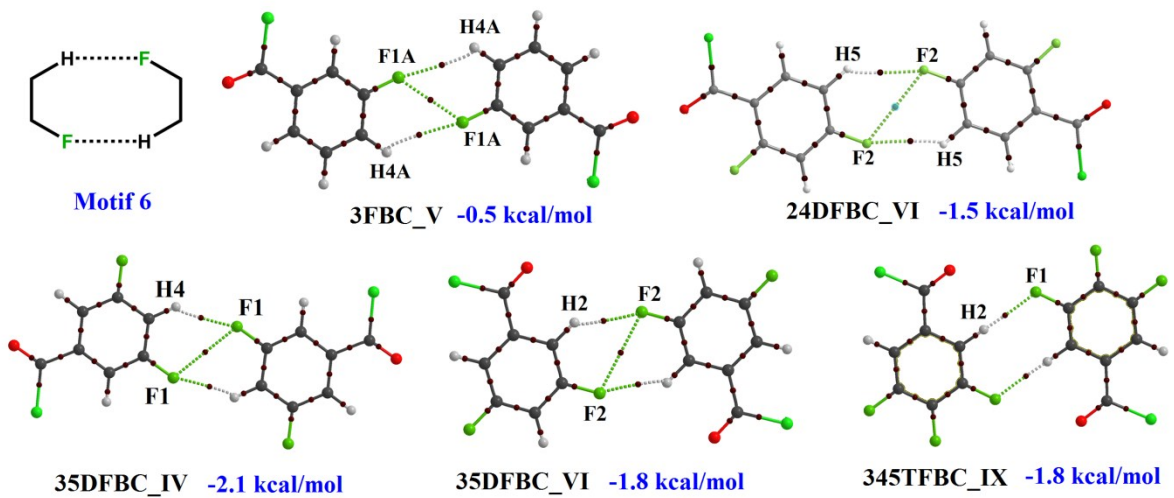


**Figure S15f.** Molecular graphs for the **Motif 6** associated with C-H···F dimer.

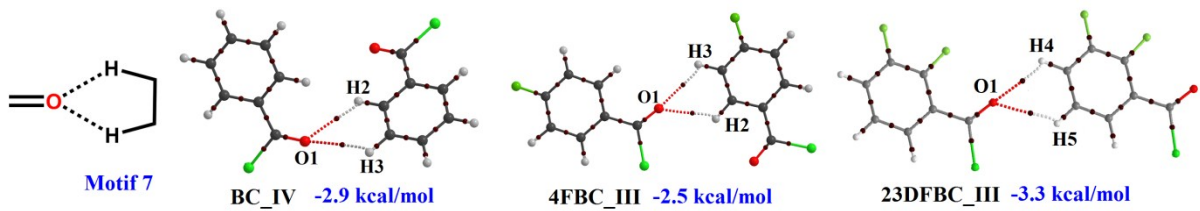


**Figure S15g.** Molecular graphs for the **Motif 7** associated with bifurcated C-H···O interaction.

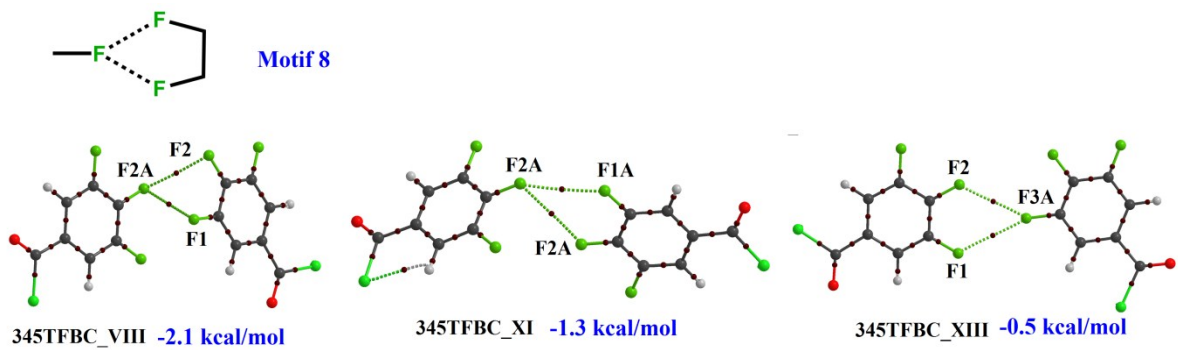


**Figure S15h.** Molecular graphs for the **Motif 8** associated with bifurcated F···F contact.

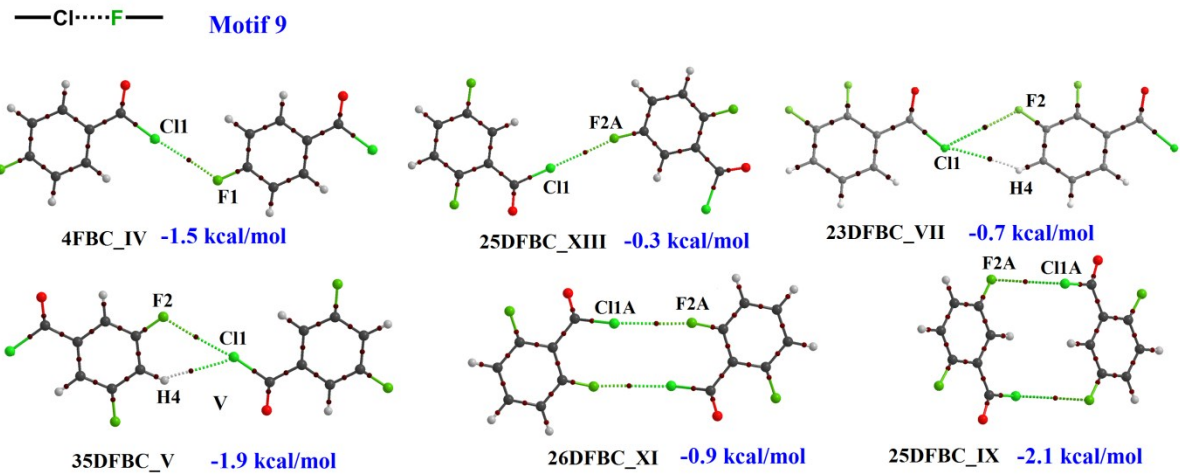


**Figure S15i.** Molecular graphs for the **Motif 9** associated with  $\text{Cl}\cdots\text{F}$  contact.

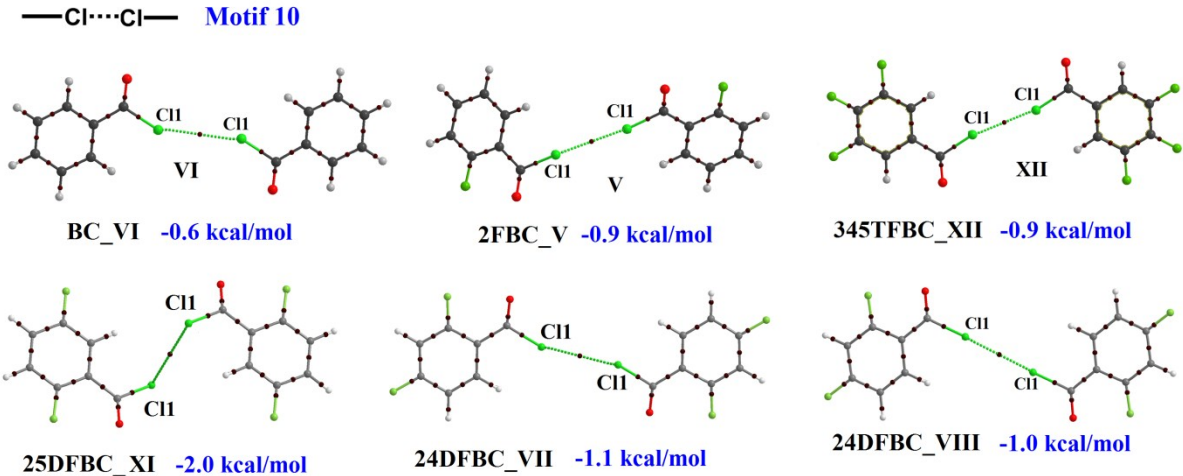


**Figure S15j.** Molecular graphs for the **Motif 10** associated with  $\text{Cl}\cdots\text{Cl}$  contact.

**Table S4.** Topological parameters for the bond critical point (BCP) of various intermolecular interactions

Motif	Molecular pair	Interactions	d(Å)	R <sub>ij</sub> (Å)	ρ <sub>BCP</sub> (e/Å <sup>3</sup> )	∇ <sup>2</sup> ρ <sub>BCP</sub> (e/Å <sup>5</sup> )	V <sub>b</sub> (a.u.)	G <sub>b</sub> (a.u.)	D.E <sup>V</sup> (kcal/mol)
1	BC_V	C4-H4···O1	2.47	2.49	0.0584	0.674	-0.005295	0.006136	1.66
	2FBC_I	C3-H3···C11	2.98	2.99	0.0354	0.399	-0.002504	0.003320	0.79
		C4-H4···O1	2.50	2.53	0.0545	0.692	-0.005145	0.006158	1.61
	3FBC_III	C4A-H4A···O1	2.73	2.77	0.0350	0.398	-0.003104	0.003614	0.97
	26DFBC_V	C3-H3···C11	3.11	3.14	0.0282	0.327	-0.001957	0.002676	0.61
		C4-H4···O1	2.45	2.47	0.0623	0.769	-0.005865	0.006922	1.84
	26DFBC_IV	C4A-H4A···C11A	2.96	2.98	0.0380	0.432	-0.002723	0.003601	0.85
		C5A-H5A···O1A	2.44	2.47	0.0638	0.775	-0.005919	0.006981	1.85
	24DFBC_III	C3-H3···C11	3.02	3.06	0.0336	0.390	-0.002362	0.003205	0.74
		C3-H3···O1	3.08	3.08	0.0232	0.320	-0.002031	0.002677	0.63
		F2···O1	3.12	3.12	0.0305	0.506	-0.003585	0.004415	1.12

2	24DFBC_IV	C3-H3···Cl1	3.10	3.02	0.0345	0.390	-0.002429	0.003236	0.76	
		F2···O1	3.06	3.07	0.0328	0.520	-0.003902	0.004646	1.22	
	345TFBC_V	F1···F2A	2.98	2.98	0.0364	0.665	-0.005076	0.005984	1.59	
3	25DFBC_VI	F2···Cl1	3.51	3.52	0.0236	0.377	-0.002055	0.002981	0.64	
		C4-H4···O1	2.60	2.62	0.0449	0.503	-0.003992	0.004603	1.25	
	25DFBC_VII	F2A···Cl1A	3.48	3.49	0.0251	0.398	-0.002224	0.003178	0.70	
		C4A-H4A···O1A	2.57	2.58	0.0476	0.537	-0.004232	0.004903	1.32	
4	35DFBC_II	Cl1···F1	3.60	3.60	0.0206	0.320	-0.001717	0.002518	0.53	
	35DFBC_III	C6-H6···O1	2.35	2.38	0.0676	0.923	-0.006461	0.008015	2.02	
5	3FBC_II	C6A-H6A···O1	2.82	2.88	0.0299	0.400	-0.002730	0.003439	0.86	
		C2A-H2A···Cl1	2.89	2.91	0.0416	0.483	-0.003063	0.004031	0.96	
	3FBC_IV	O1···F1A	2.96	2.96	0.0434	0.673	-0.005314	0.006145	1.67	
6	2FBC_II	C5-H5···O1	2.48	2.50	0.0531	0.680	-0.004995	0.006018	1.57	
		C6-H6···F1	2.57	2.62	0.0409	0.631	-0.004538	0.005539	1.42	
	2FBC_IV	C6-H6···F1	2.76	2.78	0.0277	0.415	-0.002847	0.003571	0.89	
	24DFBC_V	C6-H6···F1	2.53	2.72	0.0379	0.505	-0.003614	0.004427	1.13	
7	3FBC_V	F1A···F1A	2.66	2.65	0.0827	1.308	-0.012030	0.012787	3.77	
	24DFBC_VI	F2···F2	3.16	3.16	0.0255	0.490	-0.003167	0.004126	0.99	
		C5-H5···F2	2.61	2.64	0.0340	0.512	-0.003655	0.004483	1.14	
	35DFBC_IV	C4-H4···F1	2.45	2.49	0.0480	0.704	-0.005232	0.006266	1.64	
		F1···F1	3.11	3.12	0.0290	0.542	-0.003690	0.004654	1.15	
	35DFBC_VI	C2-H2···F2	2.54	2.58	0.0390	0.574	-0.004170	0.005063	1.31	
		F2···F2	3.26	3.26	0.0203	0.409	-0.002361	0.003302	0.74	
8	345TFBC_IX	Cl1···Cl1	3.27	3.28	0.0606	0.911	-0.005636	0.007534	1.77	
	BC_IV	C2-H2···O1	2.64	2.68	0.0443	0.559	-0.004201	0.004997	1.32	
		C3-H3···O1	2.71	2.77	0.0351	0.494	-0.003416	0.004267	1.07	
	4FBC_III	C2-H2···O1	2.55	2.65	0.0449	0.645	-0.004426	0.005552	1.39	
		C3-H3···O1	2.60	2.60	0.0545	0.706	-0.005230	0.006269	1.64	
	23DFBC_III	C4-H4···O1	2.55	2.60	0.0474	0.680	-0.004670	0.005861	1.47	
		C5-H5···O1	2.61	2.65	0.0502	0.637	-0.004782	0.005693	1.50	
9	345TFBC_VI	F1A···F2A	3.07	3.07	0.0241	0.497	-0.003259	0.004205	1.02	
		F2A···F2A	3.31	3.31	0.0154	0.342	-0.001830	0.002686	0.57	
	345TFBC_IX	Cl1···Cl1	3.27	3.28	0.0606	0.911	-0.005636	0.007534	1.77	
	345TFBC_XI	F1···F3A	2.97	2.98	0.0326	0.621	-0.004520	0.005475	1.42	
		F2···F3A	3.01	3.01	0.0288	0.567	-0.003950	0.004910	1.23	
10	4FBC_IV	F1···Cl1	3.15	3.16	0.0427	0.706	-0.004793	0.006054	1.50	
	25DFBC_XIII	Cl1···F2A	3.11	3.11	0.0401	0.711	-0.004735	0.006055	1.49	
	23DFBC_VII	Cl1···F2	3.44	3.44	0.0282	0.439	-0.002557	0.003555	0.80	
		C4-H4···Cl1	3.08	3.12	0.0247	0.317	-0.001846	0.002568	0.58	
	35DFBC_V	Cl1···F2	3.32	3.32	0.0297	0.510	-0.003026	0.004157	0.94	
		C4-H4···Cl1	2.96	2.99	0.0347	0.418	-0.002546	0.003439	0.80	
10	26DFBC_IX	Cl1···Cl1A	3.70	3.71	0.0252	0.359	-0.001742	0.002734	0.55	
	26DFBC_XI	Cl1A···F2A	3.16	3.17	0.0386	0.651	-0.004218	0.005485	1.32	
10	BC_VI	Cl1···Cl1	3.62	3.63	0.0314	0.448	-0.002265	0.003451	0.71	
	2FBC_V	Cl1···Cl1	3.52	3.53	0.0380	0.547	-0.002923	0.004295	0.92	
	345TFBC_XI_I	Cl1···Cl1	3.27		3.28	0.0606	0.911	-0.005636	0.007534	1.77
	25DFBC_XI	Cl1···Cl1	3.74	3.74	0.0333	0.390	-0.002082	0.003065	0.65	
	24DFBC_VII	Cl1···Cl1	3.43	3.64	0.0328	0.449	-0.002298	0.003476	0.72	
	24DFBC_VIII	Cl1···Cl1	3.63	3.44	0.0425	0.633	-0.003527	0.005048	1.11	

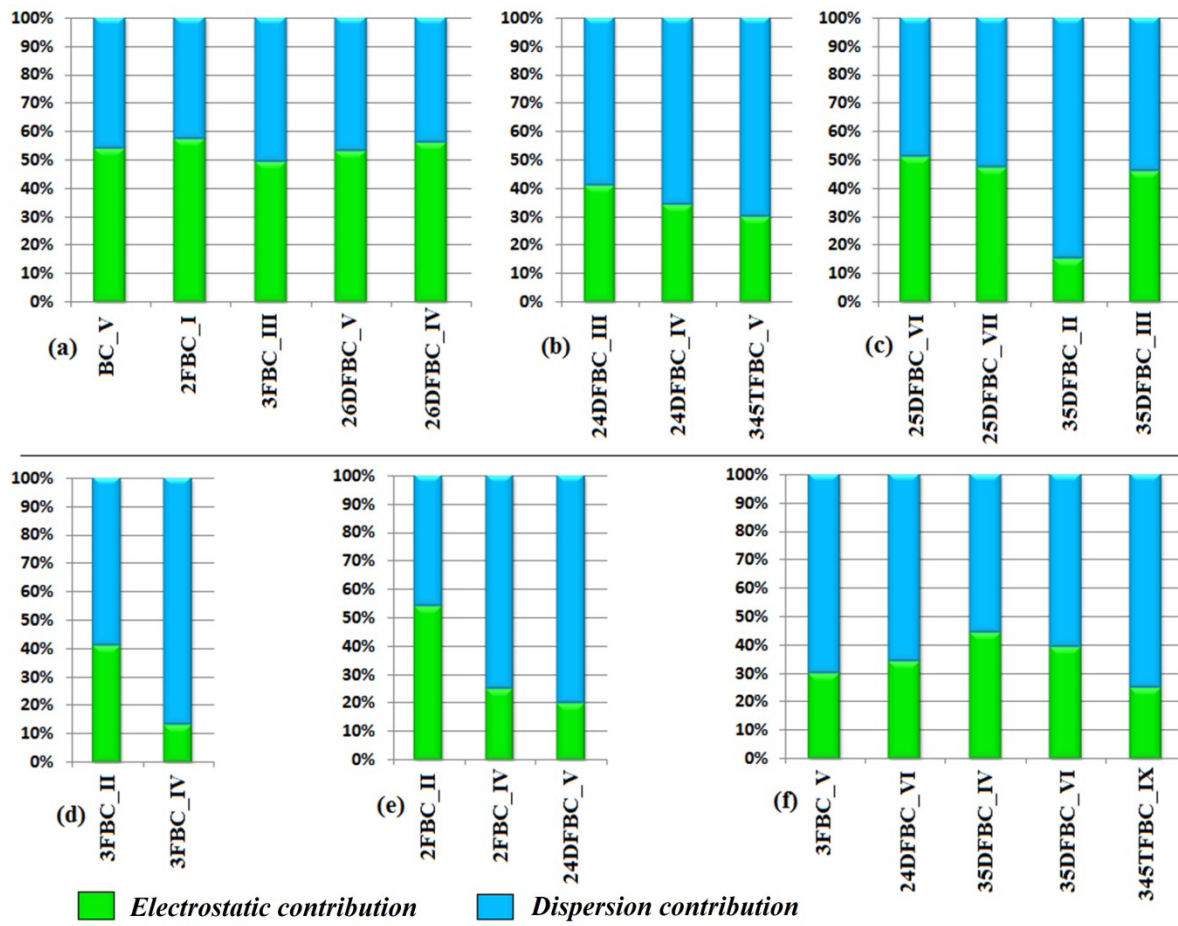


**Figure S16.** Energy distribution plot towards the total stabilization energy for the equivalent motifs (a) 1, (b) 2, (c) 3, (d) 4, (e) 5 and (f) 6.

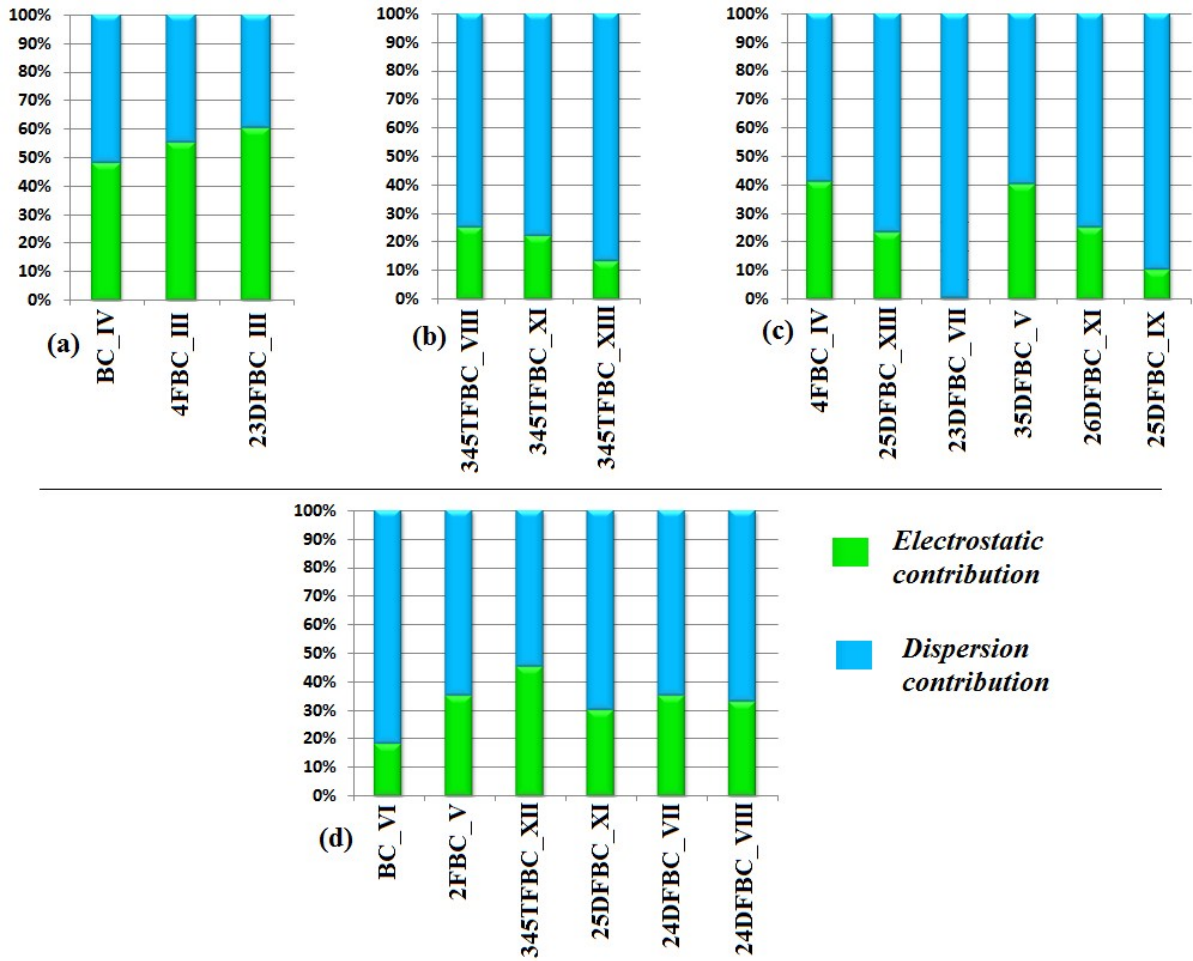


**Figure S17.** Energy distribution plot towards the total stabilization energy for the equivalent motifs (a) **7**, (b) **8**, (c) **9** and (d) **10**.

### Hirshfeld surface analysis

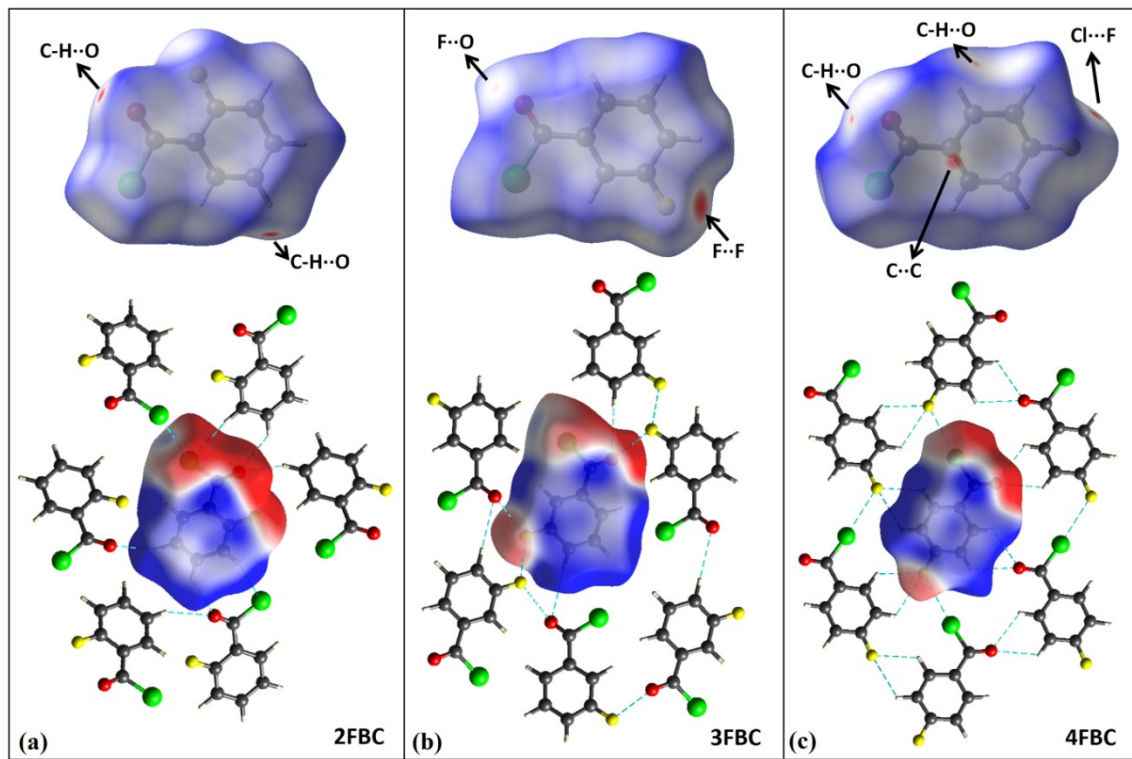


**Figure S18.** Hirshfeld surface of **2FBC**, **3FBC** and **4FBC** mapped with  $d_{\text{norm}}$  (front view and side view). ESP (Electrostatic potential) plotted on Hirshfeld surface mapped from -0.02 au (red) to 0.02 au (blue).

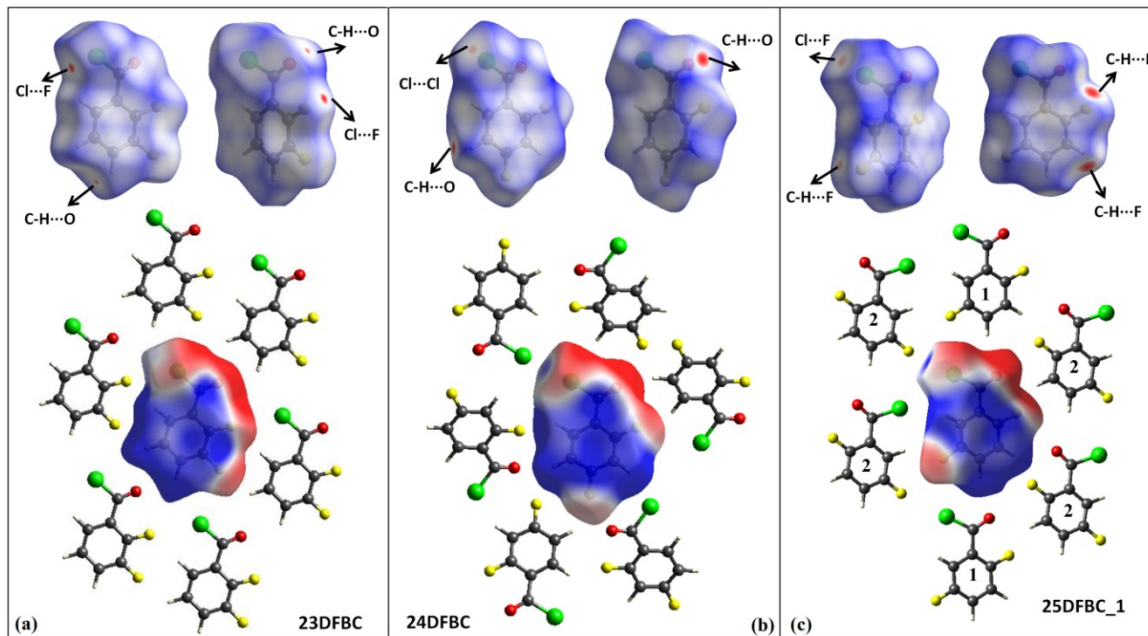


**Figure S19.** Hirshfeld surface of **23DFBC**, **24DFBC** and **25DFBC-1** mapped with  $d_{\text{norm}}$ . ESP (Electrostatic potential) plotted on Hirshfeld surface mapped from -0.02 au (red) to 0.02 au (blue).

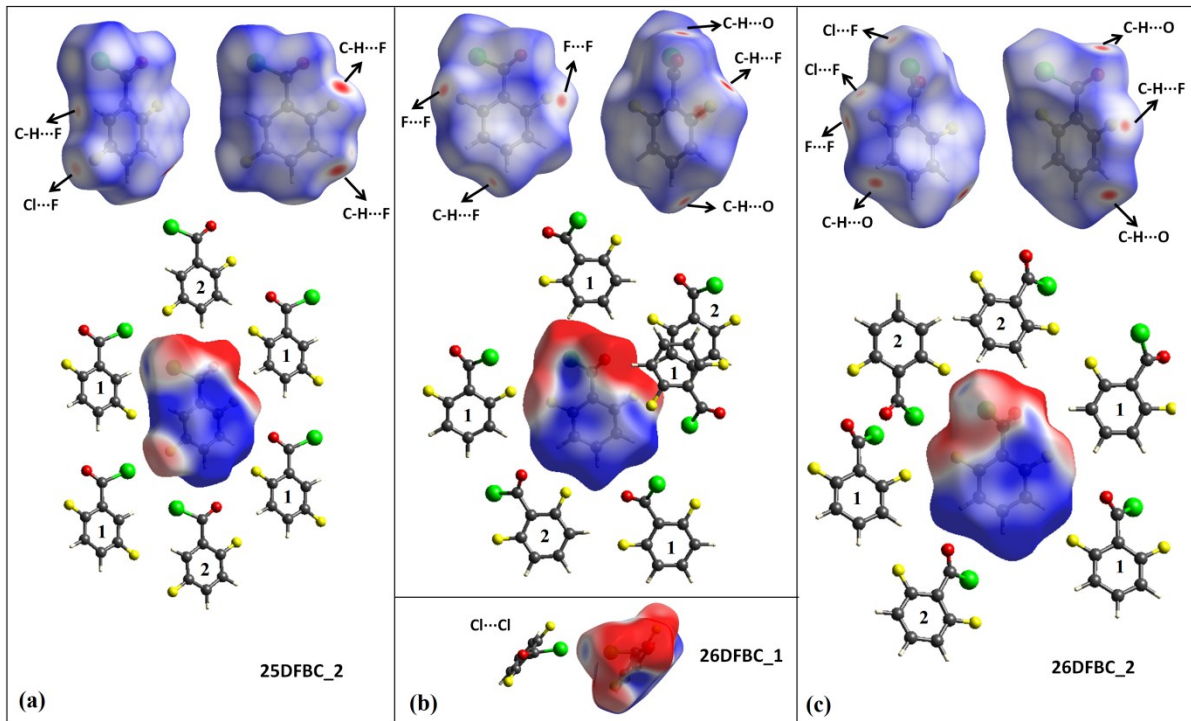


**Figure S20.** Hirshfeld surface of **25DFBC-2**, **26DFBC-1** and **26DFBC-2** mapped with  $d_{\text{norm}}$ . ESP (Electrostatic potential) plotted on Hirshfeld surface mapped from -0.02 au (red) to 0.02 au (blue).

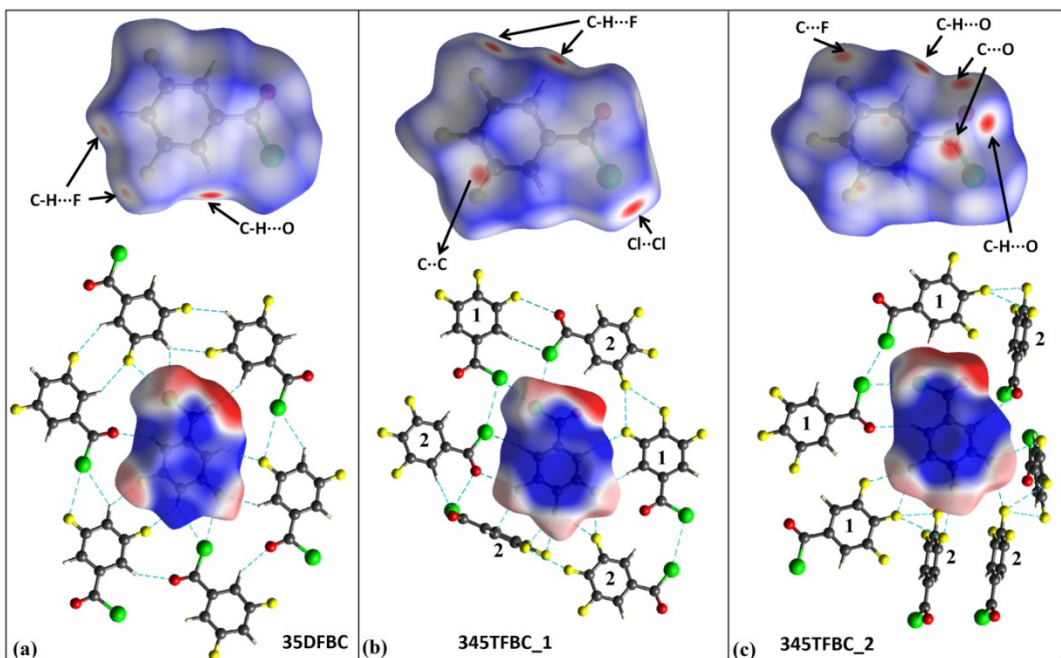


**Figure S21.** Hirshfeld surface of **35DFBC**, **345TFBC\_1** and **345TFBC\_2** mapped with  $d_{\text{norm}}$ . ESP (Electrostatic potential) plotted on Hirshfeld surface mapped from -0.02 au (red) to 0.02 au (blue).

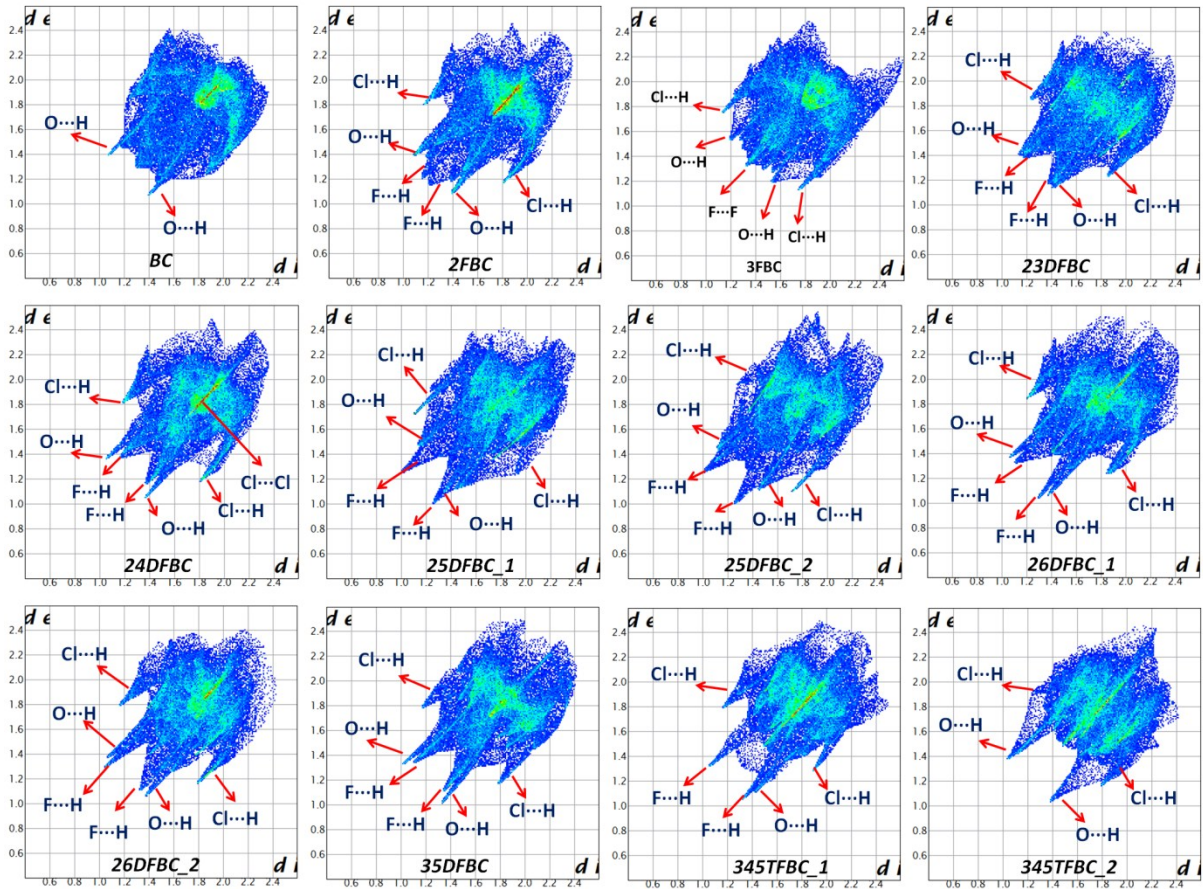


**Figure S22.** Hirshfeld surface associated fingerprint plots of fluorinated benzoyl chlorides: red arrows indicate the spikes of the respective contacts ( $\text{Cl}\cdots\text{H}$ ,  $\text{F}\cdots\text{H}$  and  $\text{O}\cdots\text{H}$ ) in the crystal packing.

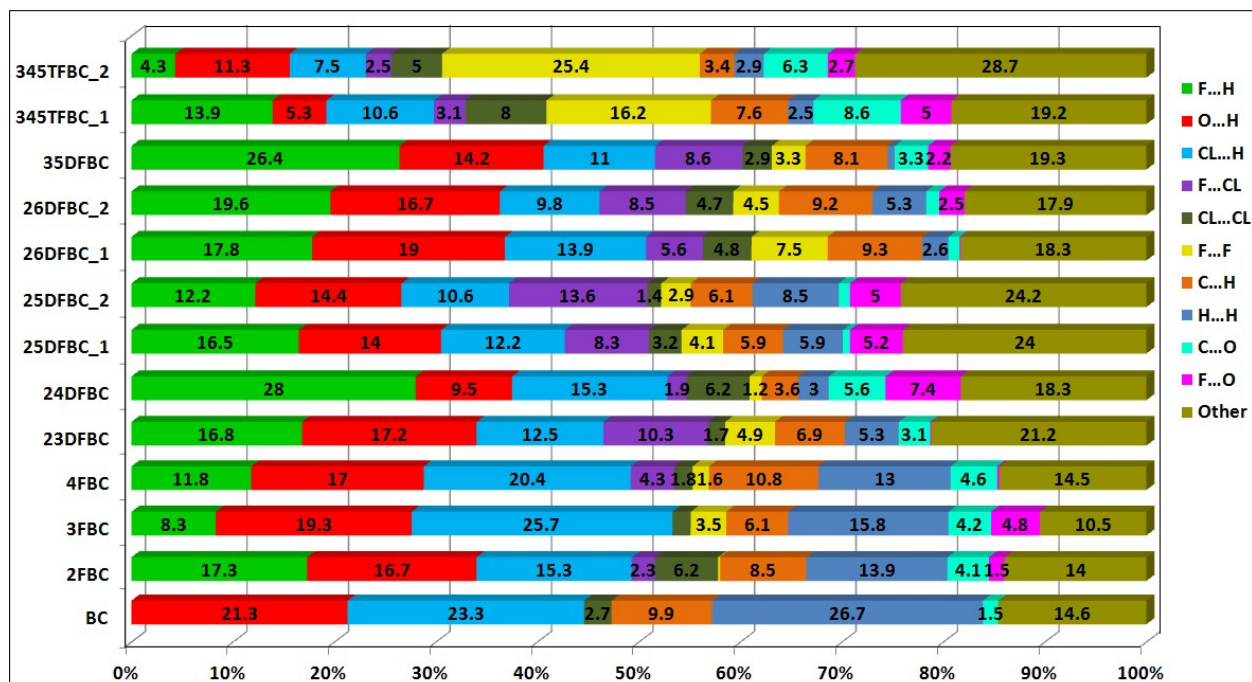


**Figure S23.** Relative contributions of different atom···atom contact in the crystal packing of fluorinated benzoyl chlorides as well as in BC.

## References

1. Apex2, Version 2 User Manual, M86-E01078, Bruker Analytical X-ray Systems Madison, WI, 2006.
2. Siemens, SMART System, Siemens Analytical X-ray Instruments Inc. Madison, MI, 1995.
3. A. Altomare, M. C. Burla, G. Camalli, G. Cascarano, C. Giacovazzo, A. Gualandi, G. Polidori, *J. Appl. Crystallogr.* 1994, **27**, 435-436.
4. G. M. Sheldrick, SADABS; Bruker AXS, Inc.: Madison, WI, 2007.
5. L. J. Farrugia, *J. Appl. Crystallogr.* 1999, **32**, 837-838.
6. G. M. Sheldrick, *Acta Crystallogr.* 2008, **A64**, 112-122.
7. C. F. Macrae, I. J. Bruno, J. A. Chisholm, P. R. Edgington, P. McCabe, E. Pidcock, L. Rodriguez-Monge, R. Taylor, J. Streek, P. A. Wood, *J. Appl. Crystallogr.* 2008, **41**, 466-470.
8. M. Nardelli, *J. Appl. Crystallogr.* 1995, **28**, 659.
9. A. L. Spek, *Acta Crystallogr.* 2009, **D65**, 148-155.
11. L. Maschio, B. Civalleri, P. Ugliengo, A. Gavezzotti, *J. Phys. Chem. A*, 2011, **115**, 11179-11186.
12. L. Carlucci, A. Gavezzotti, *Chem. Eur. J.*, 2005, **11**, 271-279.
13. M. J. Frisch, G. W. Trucks, H. B. Schlegel, G. E. Scuseria, M. A. Robb, J. R. Cheeseman, G. Scalmani, V. Barone, B. Mennucci, G. A. Petersson, H. Nakatsuji, M. Caricato, X. Li, H.

P. Hratchian, A. F. Izmaylov, J. Bloino, G. Zheng, J. L. Sonnenberg, M. Hada, M. Ehara, K. Toyota, R. Fukuda, J. M. HasegawaIshida, T. Nakajima, Y. Honda, O. Kitao, H. Nakai, T. Vreven, J. A. Jr. Montgomery, J. E. Peralta, F. Ogliaro, M. Bearpark, J. J. Heyd, E. Brothers, K. N. Kudin, V. N. Staroverov, R. Kobayashi, J. Normand, K. Raghavachari, A. Rendell, J. C. Burant, S. S. Iyengar, J. Tomasi, M. Cossi, N. Rega, J. M. Millam, M. Klene, J. E. Knox, J. B. Cross, V. Bakken, C. Adamo, J. Jaramillo, R. Gomperts, R. E. Stratmann, O. Yazyev, A. J. Austin, R. Cammi, C. Pomelli, J. W. Ochterski, R. L. Martin, K. Morokuma, V. G. Zakrzewski, G. A. Voth, P. Salvador, J. J. Dannenberg, S, Dapprich, A. D. Daniels, Ö. Farkas, J. B. Foresman, J. V. Ortiz, J. Cioslowski, D. J. Fox, Gaussian 09, Revision D.01, Gaussian, Inc., Wallingford, CT, 2009.

14. T. A. Keith, AIMALL, version 13.05.06; TK Gristmill Software, Overland Park KS, 2013; aim.tkgristmill.com.

15. I. Mata, I. Alkorta, E. Espinosa, E. Molins, *Chem. Phys. Lett.*, 2011, **507**, 185-189.

16. E. Espinosa, E. Molins, C. Lecomte, *Chem. Phys. Lett.* 1998, **285**, 170-173.